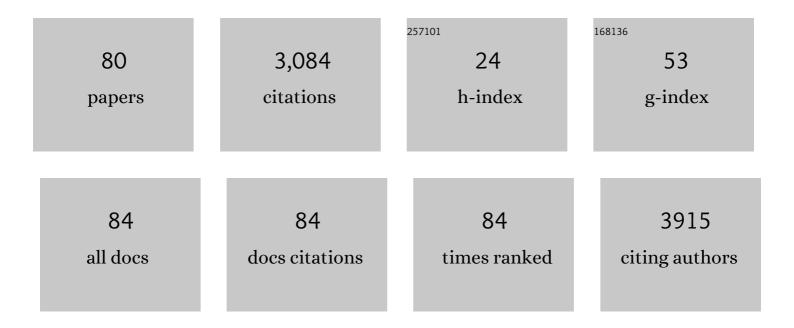
List of Publications by Year in descending order

Source: https://exaly.com/author-pdf/6209681/publications.pdf Version: 2024-02-01



ALAIN LALANDE

#	Article	IF	CITATIONS
1	Deep Learning Techniques for Automatic MRI Cardiac Multi-Structures Segmentation and Diagnosis: Is the Problem Solved?. IEEE Transactions on Medical Imaging, 2018, 37, 2514-2525.	5.4	926
2	Mutations in myosin heavy chain 11 cause a syndrome associating thoracic aortic aneurysm/aortic dissection and patent ductus arteriosus. Nature Genetics, 2006, 38, 343-349.	9.4	532
3	What are normal relaxation times of tissues at 3 T?. Magnetic Resonance Imaging, 2017, 35, 69-80.	1.0	180
4	Convolutional Neural Network With Shape Prior Applied to Cardiac MRI Segmentation. IEEE Journal of Biomedical and Health Informatics, 2019, 23, 1119-1128.	3.9	127
5	Cardiac Segmentation With Strong Anatomical Guarantees. IEEE Transactions on Medical Imaging, 2020, 39, 3703-3713.	5.4	72
6	Major prognostic impact of persistent microvascular obstruction as assessed by contrast-enhanced cardiac magnetic resonance in reperfused acute myocardial infarction. European Radiology, 2009, 19, 2117-2126.	2.3	70
7	Mapping of Familial Thoracic Aortic Aneurysm/Dissection With Patent Ductus Arteriosus to 16p12.2–p13.13. Circulation, 2005, 112, 200-206.	1.6	65
8	Time course of NAA T2 and ADCw in ischaemic stroke patients: 1H MRS imaging and diffusion-weighted MRI. Journal of the Neurological Sciences, 2004, 220, 23-28.	0.3	50
9	Familial thoracic aortic aneurysm/dissection with patent ductus arteriosus: genetic arguments for a particular pathophysiological entity. European Journal of Human Genetics, 2004, 12, 173-180.	1.4	48
10	Emidec: A Database Usable for the Automatic Evaluation of Myocardial Infarction from Delayed-Enhancement Cardiac MRI. Data, 2020, 5, 89.	1.2	46
11	3D segmentation of abdominal aorta from CT-scan and MR images. Computerized Medical Imaging and Graphics, 2012, 36, 294-303.	3.5	45
12	FCA-Net: Adversarial Learning for Skin Lesion Segmentation Based on Multi-Scale Features and Factorized Channel Attention. IEEE Access, 2019, 7, 130552-130565.	2.6	45
13	Influence of age and sex on aortic distensibility assessed by MRI in healthy subjects. Magnetic Resonance Imaging, 2010, 28, 255-263.	1.0	42
14	MR Imaging of the Heart in Patients after Myocardial Infarction: Effect of Increasing Intersection Gap on Measurements of Left Ventricular Volume, Ejection Fraction, and Wall Thickness. Radiology, 1999, 213, 513-520.	3.6	41
15	Automatic segmentation of tumors and affected organs in the abdomen using a 3D hybrid model for computed tomography imaging. Computers in Biology and Medicine, 2020, 127, 104097.	3.9	32
16	Automatic Detection of Left Ventricular Contours from Cardiac Cine Magnetic Resonance Imaging Using Fuzzy Logic. Investigative Radiology, 1999, 34, 211-217.	3.5	31
17	The extent of myocardial damage assessed by contrast-enhanced MRI is a major determinant of N-BNP concentration after myocardial infarction. European Journal of Heart Failure, 2004, 6, 555-560.	2.9	30
18	Learning With Context Feedback Loop for Robust Medical Image Segmentation. IEEE Transactions on Medical Imaging, 2021, 40, 1542-1554.	5.4	30

#	Article	IF	CITATIONS
19	Nonsupervised Ranking of Different Segmentation Approaches: Application to the Estimation of the Left Ventricular Ejection Fraction From Cardiac Cine MRI Sequences. IEEE Transactions on Medical Imaging, 2012, 31, 1651-1660.	5.4	27
20	Contribution of Augmented Reality to Minimally Invasive Computer-Assisted Cranial Base Surgery. IEEE Journal of Biomedical and Health Informatics, 2019, 24, 1-1.	3.9	27
21	Automatic Determination of Aortic Compliance With Cine-Magnetic Resonance Imaging. Investigative Radiology, 2002, 37, 685-691.	3.5	26
22	Visual estimation of the global myocardial extent of hyperenhancement on delayed contrast-enhanced MRI. European Radiology, 2004, 14, 2182-2187.	2.3	26
23	An Adapted Optical Flow Algorithm for Robust Quantification of Cardiac Wall Motion From Standard Cine-MR Examinations. IEEE Transactions on Information Technology in Biomedicine, 2012, 16, 859-868.	3.6	26
24	Relationship Between Fragmented QRS and No-Reflow, Infarct Size, and Peri-Infarct Zone Assessed Using Cardiac Magnetic Resonance in Patients With Myocardial Infarction. Canadian Journal of Cardiology, 2014, 30, 204-210.	0.8	26
25	Congenital Complete Absence of the Left Pericardium: A Rare Cause of Chest Pain or Pseudoâ€right Heart Overload. Clinical Cardiology, 2010, 33, E52-7.	0.7	24
26	Cardiac MRI Segmentation with Strong Anatomical Guarantees. Lecture Notes in Computer Science, 2019, , 632-640.	1.0	24
27	Fast interactive medical image segmentation with weakly supervised deep learning method. International Journal of Computer Assisted Radiology and Surgery, 2020, 15, 1437-1444.	1.7	23
28	A deep learning method for real-time intraoperative US image segmentation in prostate brachytherapy. International Journal of Computer Assisted Radiology and Surgery, 2020, 15, 1467-1476.	1.7	22
29	Semiautomatic detection of myocardial contours in order to investigate normal values of the left ventricular trabeculated mass using MRI. Journal of Magnetic Resonance Imaging, 2016, 43, 1398-1406.	1.9	21
30	Augmented Reality of the Middle Ear Combining Otoendoscopy and Temporal Bone Computed Tomography. Otology and Neurotology, 2018, 39, 931-939.	0.7	21
31	Generative Adversarial Networks in Cardiology. Canadian Journal of Cardiology, 2022, 38, 196-203.	0.8	21
32	Use of Super Paramagnetic Iron Oxide Nanoparticles as Drug Carriers in Brain and Ear: State of the Art and Challenges. Brain Sciences, 2021, 11, 358.	1.1	19
33	Microtubule alteration is an early cellular reaction to the metabolic challenge in ischemic cardiomyocytes. Molecular and Cellular Biochemistry, 2004, 258, 99-108.	1.4	18
34	Prognostic Value of Microvascular Damage Determined by Cardiac Magnetic Resonance in Non ST-Segment Elevation Myocardial Infarction. Investigative Radiology, 2010, 45, 725-732.	3.5	17
35	Left Ventricular Ejection Fraction Calculation from Automatically Selected and Processed Diastolic and Systolic Frames in Short?Axis Cine?MRI. Journal of Cardiovascular Magnetic Resonance, 2004, 6, 817-827.	1.6	16
36	Deep learning methods for automatic evaluation of delayed enhancement-MRI. The results of the EMIDEC challenge. Medical Image Analysis, 2022, 79, 102428.	7.0	16

#	Article	IF	CITATIONS
37	Video-based augmented reality combining CT-scan and instrument position data to microscope view in middle ear surgery. Scientific Reports, 2020, 10, 6767.	1.6	15
38	Utility of Cardiac Magnetic Resonance to assess association between admission hyperglycemia and myocardial damage in patients with reperfused ST-Segment Elevation Myocardial Infarction. Journal of Cardiovascular Magnetic Resonance, 2008, 10, 2.	1.6	13
39	Graph cut-based method for segmenting the left ventricle from MRI or echocardiographic images. Computerized Medical Imaging and Graphics, 2017, 58, 1-12.	3.5	13
40	Automatic segmentation of inner ear on CT-scan using auto-context convolutional neural network. Scientific Reports, 2021, 11, 4406.	1.6	13
41	A novel alternative to classify tissues from T 1 and T 2 relaxation times for prostate MRI. Magnetic Resonance Materials in Physics, Biology, and Medicine, 2016, 29, 777-788.	1.1	12
42	Comparison of the Extent of Delayed-Enhancement Cardiac Magnetic Resonance Imaging With and Without Phase-Sensitive Reconstruction at 3.0 T. Investigative Radiology, 2007, 42, 372-376.	3.5	11
43	Improved Estimation of Cardiac Function Parameters Using a Combination of Independent Automated Segmentation Results in Cardiovascular Magnetic Resonance Imaging. PLoS ONE, 2015, 10, e0135715.	1.1	11
44	Exercise stress CMR reveals reduced aortic distensibility and impaired right-ventricular adaptation to exercise in patients with repaired tetralogy of Fallot. PLoS ONE, 2018, 13, e0208749.	1.1	11
45	Augmented reality for inner ear procedures: visualization of the cochlear central axis in microscopic videos. International Journal of Computer Assisted Radiology and Surgery, 2020, 15, 1703-1711.	1.7	11
46	Realignment of myocardial first-pass MR perfusion images using an automatic detection of the heart-lung interface. Magnetic Resonance Imaging, 2004, 22, 1001-1009.	1.0	9
47	Comparison of the strain field of abdominal aortic aneurysm measured by magnetic resonance imaging and stereovision: A feasibility study for prediction of the risk of rupture of aortic abdominal aneurysm. Journal of Biomechanics, 2015, 48, 1158-1164.	0.9	9
48	Myocardial Infarction Quantification from Late Gadolinium Enhancement MRI Using Top-Hat Transforms and Neural Networks. Algorithms, 2021, 14, 249.	1.2	9
49	Aortic Function's Adaptation in Response to Exercise-Induced Stress Assessing by 1.5T MRI: A Pilot Study in Healthy Volunteers. PLoS ONE, 2016, 11, e0157704.	1.1	9
50	Inferring postimplant dose distribution of salvage permanent prostate implant (PPI) after primary PPI on CT images. Brachytherapy, 2018, 17, 866-873.	0.2	8
51	Deep Generative Model-Driven Multimodal Prostate Segmentation in Radiotherapy. Lecture Notes in Computer Science, 2019, , 119-127.	1.0	8
52	Measurement of the local aortic stiffness by a non-invasive bioelectrical impedance technique. Medical and Biological Engineering and Computing, 2011, 49, 431-439.	1.6	7
53	Validation of the Strain Assessment of a Phantom of Abdominal Aortic Aneurysm: Comparison of Results Obtained From Magnetic Resonance Imaging and Stereovision Measurements. Journal of Biomechanical Engineering, 2018, 140, .	0.6	7
54	Automatic classification of tissues on pelvic MRI based on relaxation times and support vector machine. PLoS ONE, 2019, 14, e0211944.	1.1	7

#	Article	IF	CITATIONS
55	Deep Learning–based Automated Segmentation of Left Ventricular Trabeculations and Myocardium on Cardiac MR Images: A Feasibility Study. Radiology: Artificial Intelligence, 2021, 3, e200021.	3.0	7
56	Aortic local biomechanical properties in ascending aortic aneurysms. Acta Biomaterialia, 2022, 149, 40-50.	4.1	7
57	Automatic Fuzzy Classification of the Washout Curves From Magnetic Resonance First-Pass Perfusion Imaging After Myocardial Infarction. Investigative Radiology, 2005, 40, 545-555.	3.5	6
58	ProstateAnalyzer: web-based medical application for the management of prostate cancer using multiparametric MR imaging. Informatics for Health and Social Care, 2015, 41, 1-21.	1.4	6
59	Left-Ventricle Segmentation of SPECT Images of Rats. IEEE Transactions on Biomedical Engineering, 2015, 62, 2260-2268.	2.5	5
60	MedicalSeg: A Medical GUI Application for Image Segmentation Management. Algorithms, 2022, 15, 200.	1.2	5
61	Automatic evaluation of the Valsalva sinuses from cine-MRI. Magnetic Resonance Materials in Physics, Biology, and Medicine, 2011, 24, 359-370.	1.1	4
62	Automatic deformable PET/MRI registration for preclinical studies based on B-splines and non-linear intensity transformation. Medical and Biological Engineering and Computing, 2018, 56, 1531-1539.	1.6	4
63	Semi-automatic detection of myocardial trabeculation using cardiovascular magnetic resonance: correlation with histology and reproducibility in a mouse model of non-compaction. Journal of Cardiovascular Magnetic Resonance, 2018, 20, 70.	1.6	4
64	Comparison of different segmentation approaches without using gold standard. Application to the estimation of the left ventricle ejection fraction from cardiac cine MRI sequences. , 2011, 2011, 2663-6.		3
65	Comparison of two techniques (in vivo and ex-vivo) for evaluating the elastic properties of the ascending aorta: Prospective cohort study. PLoS ONE, 2021, 16, e0256278.	1.1	3
66	More than 50% of Persistent Myocardial Scarring at One Year in "Infarct-like―Acute Myocarditis Evaluated by CMR. Journal of Clinical Medicine, 2021, 10, 4677.	1.0	3
67	Augmented Reality Based Transmodiolar Cochlear Implantation. Otology and Neurotology, 2021, Publish Ahead of Print, .	0.7	3
68	Automatic Myocardial Infarction Evaluation from Delayed-Enhancement Cardiac MRI Using Deep Convolutional Networks. Lecture Notes in Computer Science, 2021, , 378-384.	1.0	2
69	Vision-Based Augmented Reality System for Middle Ear Surgery: Evaluation in Operating Room Environment. Otology and Neurotology, 2022, 43, 385-394.	0.7	2
70	Usefulness of Collaborative Work in the Evaluation of Prostate Cancer from MRI. Clinics and Practice, 2022, 12, 350-362.	0.6	2
71	Automatic evaluation of the sinus of Valsalva from cine-MRI in patients with dilated aortic root. Journal of Cardiovascular Magnetic Resonance, 2011, 13, .	1.6	1
72	Automatic measurement of the sinus of Valsalva by image analysis. Computer Methods and Programs in Biomedicine, 2017, 148, 123-135.	2.6	1

#	Article	IF	CITATIONS
73	Impact of ascending aorta replacement by graft on elastic properties of descending thoracic aorta evaluated by cardiac magnetic resonance imaging. Magnetic Resonance Materials in Physics, Biology, and Medicine, 2020, 33, 641-647.	1.1	1
74	A deep learning approach for the segmentation of myocardial diseases. , 2021, , .		1
75	Deep Learning Based Cardiac MRI Segmentation: Do We Need Experts?. Algorithms, 2021, 14, 212.	1.2	1
76	Deep Learning Techniques for Automatic MRI Cardiac Multi-Structures Segmentation and Diagnosis: Is the Problem Solved?. , 0, .		1
77	Curvilinear Multiplanar Reconstruction to Predict Useful Length and Diameter of Cochlear Lumen for Cochlear Implantation. Otology and Neurotology, 2020, 41, e1207-e1213.	0.7	1
78	A 3D deep learning approach based on Shape Prior for automatic segmentation of myocardial diseases. , 2020, , .		1
79	Efficient 3D Deep Learning for Myocardial Diseases Segmentation. Lecture Notes in Computer Science, 2021, , 359-368.	1.0	0
80	Segmentation-Free Estimation of Aortic Diameters from MRI Using Deep Learning. Lecture Notes in Computer Science, 2021, , 166-174.	1.0	0